Microbead QD-ELISA: Microbead ELISA Using Biocatalytic Formation of Quantum Dots for Ultra High Sensitive Optical and Electrochemical Detection

*Ruta Grinyte, Javier Barroso, Marco Möller, Laura Saa, Valeri Pavlov**

CIC biomaGUNE, Paseo de Miramón 182, 20009 Donostia-San Sebastián, Spain.

KEYWORDS: quantum dots, microbeads, immunoassay, electrochemistry, SOD2

ABSTRACT

Electrochemical detection strategies employing semiconductor quantum dots (QDs) open up new opportunities for highly sensitive detection of biological targets. We designed new a assay based on microbead linked enzymatic generation of CdS QDs (Microbead QD-ELISA) and employed it in optical and electrochemical affinity assays for the cancer biomarker superoxide dismutase 2 (SOD2). Biotinylated antibodies against SOD2 were immobilized on the surface of polyvinyl chloride microbeads bearing streptavidin. In order to prevent any non specific adsorption the microbeads were further blocked with bovine serum albumin. The analyte, SOD2 was captured on microbeads and labeled with alkaline phosphatase-conjugated antibody linked

with mouse antibody against SOD2. Hydrolysis of para-nitrophenylphosphate by immobilized alkaline phosphatase triggered the rapid formation of phosphate-stabilized CdS QDs on the surface of microbeads. The resulting semiconductor nanoparticles were detected by fluorescence spectroscopy, microscopy and square-wave voltammetry (SWV). The electrochemical assay based on the detection with square-wave voltammograms of Cd^{2+} ions originating from immobilized CdS QDs showed linearity up to 45 ng mL^{-1}, and the limit of SOD2 detection equal to 0.44 ng mL^{-1} (1.96 x 10^{-11} M). This detection limit is lower by two orders of magnitude in comparison with that of other previously published assays for superoxide dismutase. The electrochemical assay was validated with HepG2 (Human hepatocellular carcinoma) cell lysate containing SOD2.

INTRODUCTION

Biochemical assays use specific chemical interaction to detect target analytes by different recognition elements such as antibodies (in immunoassays),[1] DNA (deoxyribonucleic acid) aptamers,[2, 3] or nanostructured imprinted polymer films.[4, 5] Immunoassays have been broadly applied to a variety of platforms, including microtiter plate based immunoassays, lateral flow immunochromatographic assays and bead-based immunoassays. The enzyme-linked immunosorbent assay (ELISA) relying on enzymes like horseradish peroxidase (HRP) or alkaline phosphatase (ALP) for signal amplification is probably the most ubiquitous bioanalysis method used in clinical diagnostics for diagnosis of infectious diseases, food allergen detection and plant pathogens.[6-9]

Microparticles are commonly used as a solid support for the immobilization of recognition elements in immunoreactions[10] in order to capture and separate target molecules and thus are also used in conjunction with ELISA. The bead-based ELISA originates from sandwich ELISA and substitutes the flat plastic surface supports with magnetic, polymeric beads or microspheres. Due to the mobility of the particles, bead-based ELISA can be applied in more detection systems.[11-14] Traditionally, the detection of the enzyme labels was performed by optical assays based on chromogenic and fluorogenic organic substrates, which change absorption or emission spectra in the course of enzymatic reactions. However, most of the organic dyes currently in use for bead-based ELISA are not very resistant against decomposition under the action of light in the presence of oxygen, hydrogen peroxide and water in the assay mixture resulting in bleaching. Metal nanoparticles (NPs) demonstrate much higher stability, and due to their high extinction coefficients they are increasingly finding application in bioanalysis, for instance by triggering the formation of detectable metal NPs by an enzymatic reaction chain involving glucose oxidase (GOx), ALP or alcohol dehydrogenase (AlcDH).[15-19] However, metal NPs produced by the enzymes are not fluorescent and rarely demonstrate photocatalytic activities, and therefore their use in bioapplications is limited. In contrast, semiconductor NPs show the intrinsic capacity to become photoexcited and subsequently emit fluorescent light in the relaxation process. Quantum effects govern this behavior, and therefore these particles are referred to in the literature as quantum dots (QDs). The wavelength and intensity of the emitted light is defined by the chemical composition and the shape of the QDs, and also by its environment, which makes them a very interesting target for a wider application in bioassays.[20]

Our group has pioneered the enzymatic *in situ* growth[21-25] and etching [26] of fluorescent semiconductor CdS QDs, and on this base developed fluorogenic enzymatic assays. Those

assays were much more cost efficient, lower production time and demonstrated lower detection limits and better sensitivities than the standard assays based on organic substrates.[20] The general methodology can now be readily applied to any bioassay using enzymes for signal amplification. We applied this technique to a traditional optical ELISA test where biocatalytic growth of fluorescent CdS QDs was used for the detection of an analyte captured on the surface of polystyrene microplates.[27]

While the exploitation of the optical properties of QDs is usually a key parameter in the design of such ultra sensitive assays, there is still little knowledge about the practical exploitation of a pure electrochemical (without the need of any light source and optical detector) quantification of enzymatically generated QDs. Usually, the metal ions (Cd^{2+}, Pb^{2+}, Zn^{2+}) of semiconductor NPs possess different oxidation potentials yielding well-resolved voltammetric signals with a nicely low detection limit, [28-32] and works by Bard et al. showed that in particular CdS QDs exhibit the requested inherent electrochemical properties which are necessary for an electrochemical detection.[33, 34]

In recent years, several voltammetric techniques such as linear sweep, differential pulse voltammetry (DPV) and square-wave voltammetry (SWV) have been the most widely employed electrochemical methods for characterization and quantification of QDs.[35, 36] SWV became the most employed methodology due to its high selectivity and sensitivity.[28-32] The inexpensive, commercially available, disposable screen-printed electrodes (SPEs) with their versatility, miniaturization and ease of handling[37, 38] significantly diminish assay times and volume samples, being therefore increasingly used.

To the best of our knowledge the electrochemical detection of biocatalytically generated QDs has neither been reported nor applied to bioanalysis. On the other hand, the enzymatic formation

and deposition of QDs on microbeads with analytical applications has never been reported. In situ deposition of CdS QDs by the amplifying enzyme ALP potentially can yield very sensitive electrochemical assays due to the fact that one enzyme can generate several CdS QDs. In this study, we developed a methodology for the direct detection of enzymatically generated CdS QDs captured on microbeads which subsequently were subjected to an acid attack. The released cadmium ions were monitored by SWV using SPEs.

If the exploitation of an electrochemical quantification of QDs in an enzymatically amplified bioassay would turn out to be less expensive than fluorometry, then we could offer a quite universal bioanalytical platform using the enzymatic growth of QDs It would finally be applicable to an extremely wide range of detection systems, spanning from optical laboratory equipment to perspective low power requiring microfluidic systems (in which even the final washing step can be automated) and thus fast point of care (POC) analysis systems.

We applied the developed electrochemical Microbead QD-ELISA to the detection of the important biomarker superoxide dismutase 2 (SOD2) and compared the assay performance with that of the relevant fluorogenic and chromogenic affinity bioassays.

SOD2 is an antioxidant enzyme which catalyzes the dismutation of superoxide anion into molecular oxygen and hydrogen peroxide. This enzyme protects cells against reactive free radicals by neutralizing superoxide anions produced under oxidative conditions.[39] Numerous studies have demonstrated over-expression of SOD2 in various types of cancer cells like breast cancer, pancreatic adenocarcinoma, papilloma, prostate carcinoma and other cancer cells.[40-43] Measurement of the SOD2 concentration in cells is essential for monitoring the clinical course of the disease and distinguishing between the different stages of tumors. In this study, we applied our system to analysis of SOD2 in Human hepatocellular carcinoma (HepG2) cells lysate.

EXPERIMENTAL SECTION

Material and reagents. Bovine serum albumin (BSA), antimouse Immunoglobulin G (IgG)-(whole molecule)-ALP, sodium sulfide (Na_2S), cadmium nitrate $Cd(NO_3)_2$, 4-nitrophenyl phosphate disodium salt (pNPP) and other chemicals were supplied by Sigma-Aldrich. Human SOD2 full length protein, anti-SOD2 antibody-biotin (developed in rabbit), anti-SOD2 antibody (developed in mouse), HepG2 whole cell lysate were purchased from Abcam. 1 µm diameter polyvinyl chloride microbeads decorated with streptavidin (beadBALL-Streptavidin®) were purchased from Chemicell (Germany). Screen-printed electrodes (SPEs) were purchased from DropSens (Spain). Disposable customized devices based on a single-working carbon electrode, carbon counter electrode and Ag/AgCl reference electrode were specially designed to work with microvolumes of a sample. The stability of the Ag/AgCl reference electrode was confirmed by performing cyclic voltammetry with $K_3[Fe(CN)_6]$. A boxed connector (DropSens) was employed as interface between SPEs and potentiostat.

Preparation of polyvinyl chloride microspheres/antiSOD2 composites. 100 µL of polyvinyl chloride microbeads-streptavidin (10 mg mL^{-1}) were added into a clean 0.5 mL microcentrifuge tube and centrifuged at 500 x g for 1 min. The supernatant was discarded, and 100 µL of Tris-buffered saline, pH 8.0 (TBS) buffer were added to the beads. The beads were spun down and resuspended into 50 µL of buffer, and 50 µL of anti-SOD2 antibody-biotin (0.1 mg mL^{-1}) were added to the solution. The concentration of SOD2 antibody-biotin equal to 0.1 mg mL^{-1} was suggested by the standard protocol of Chemicell for immobilization of biotinylated antibodies. After 15 min incubation the beads were washed 3 times with 100 µL of TBS and resuspended in 100 µL of buffer. To prevent nonspecific binding of proteins microbeads were blocked by incubation with 5 % (w/v) BSA in TBS, overnight at 4 ^{o}C. Then beads were washed three times

with TBS/0.05 % (v/v) Tween20® (TBST) and resuspended in the same buffer to a final volume of 100 µL.

Detection of SOD2 protein by fluorogenic and chromogenic methods. 20 µL of prepared beads were incubated for 1 hour in samples of different concentration of SOD2 protein in TBS, final volume 100 µL. The microbeads were washed 3 times with 200 µL TBST. The mixture of microbeads, anti-SOD2 antibody (1:10) and antimouse-ALP (1:100) in TBS was agitated in the microcentrifuge tube for 1 h at room temperature (RT). The beads were then washed three times with TBST and once with Tris buffer (50 mM Tris-HCl buffer and 1 mM $MgCl_2$, pH 8.8). Then, 90 µL of ALP substrate (0.56 mM pNPP in 50 mM Tris-HCl buffer and 1 mM $MgCl_2$, pH 8.8) was added to each sample and incubated for 30 min at RT. Afterwards, 5 µL of 1 mM Na_2S and 5 µL of 50 mM $Cd(NO_3)_2$ were added. After incubation of 30 min the beads were washed once with 100 µL Tris buffer (50 mM Tris-HCl buffer and 1 mM $MgCl_2$, pH 8.8) and placed to a black 96-well NUNC® microtiter plate. The fluorescence emission spectra of the resulting suspension were recorded at λ_{ex} = 320 nm. For ALP substrate detection by the standard chromogenic method, the supernatant obtained after washing was transferred into transparent flat-well NUNC® 96-well microtiter plates. The absorbance at λ = 410 nm was measured. Furthermore, the fluorescence spectra for the detection of spiked SOD2 (3 µg mL^{-1}) in real samples (HepG2 whole cell lysate) was measured.

Release of free cadmium ions from adsorbed CdS NPs. 100 µL aliquots of microbeads samples bearing enzymatically produced CdS NPs obtained in the above mentioned experiment were placed into Amicon® Ultra-0.5 centrifugal filters (3000 NMWL) and washed 3 times with Tris-HCl buffer (10mM, pH 8.8). Finally, the recovered mixtures were transferred into new

filters and 200 µL of 0.2 M HCl was added to release Cd^{2+} cations from the captured CdS NPs. After centrifugation, the cadmium solutions were transferred to the pretreated SPEs.

Electrochemical detection. Before SWV measurements SPEs were pretreated electrochemically by cyclic voltammetry (CV) for 20 cycles at a potential range of 0 – 1 V in Tris-HCl buffer (10 mM, pH 8.8). Subsequently, a 40 µL drop of collected solutions was placed on the SPEs and electrochemical SWV measurements were conducted by electrodepositing cadmium at -1.2 V for 2 minutes and stripping from -1.2 to -0.6 V. The square wave parameters mainly included 2 mV step potential, 25 mV amplitude and 25 Hz frequency.

In order to follow the the quality of the washing of CdS NPs adsorbed on microbeads from exogenous Cd^{2+} ions, the collected waste solution was measured by SWV after each washing step (**Figure S1** Supporting Information).

All electrochemical data was recorded on the Autolab Electrochemical Workstation (Model: PGSTAT302N, Metrohm Autolab, The Netherlands) equipped with NOVA 1.10 software. All experiments were performed at room temperature. Unless mentioned otherwise, all experimental results presented here are averaged from three independent measurements (n = 3).

RESULTS AND DISCUSSION

Scheme 1 outlines the model assay for detection of SOD2 by enzymatic generation of CdS QDs. The stages of modification of polyvinyl chloride microbeads with antiSOD2 are shown in Scheme 1A. Briefly, streptavidin coated microbeads were mixed with polyclonal biotin labeled capture antibodies specific to SOD2 protein. To avoid nonspecific adsorption of interfering species on the surface of the beads 5% (w/v) BSA was used to block the surface. The stages of the bioassay for SOD2 are presented in Scheme 1B. It describes microbead-based ELISA for detection of SOD2 protein. Previously prepared blocked polyvinyl chloride microbeads bearing

capture antiSOD2 were incubated in sample solutions containing different concentrations of SOD2 protein. Next, detecting anti-SOD2 antibody from mouse was specifically bound to SOD2 protein on the microbead surface. Secondary ALP-conjugated antimouse IgG was added to label the Fc region of immobilized mouse anti-SOD2 detecting antibody. The microbeads were washed to remove the unbound secondary antibody-enzyme conjugates.

Scheme 1. The Principle of Microbead-Based ELISA. (A) Procedure of Microbeads Bearing Anti-SOD2 and BSA; (B) Immobilization of ALP Mediated by the Analyte; (C) The Biocatalytic Signal Amplification Cascade for Detection of Analyte.

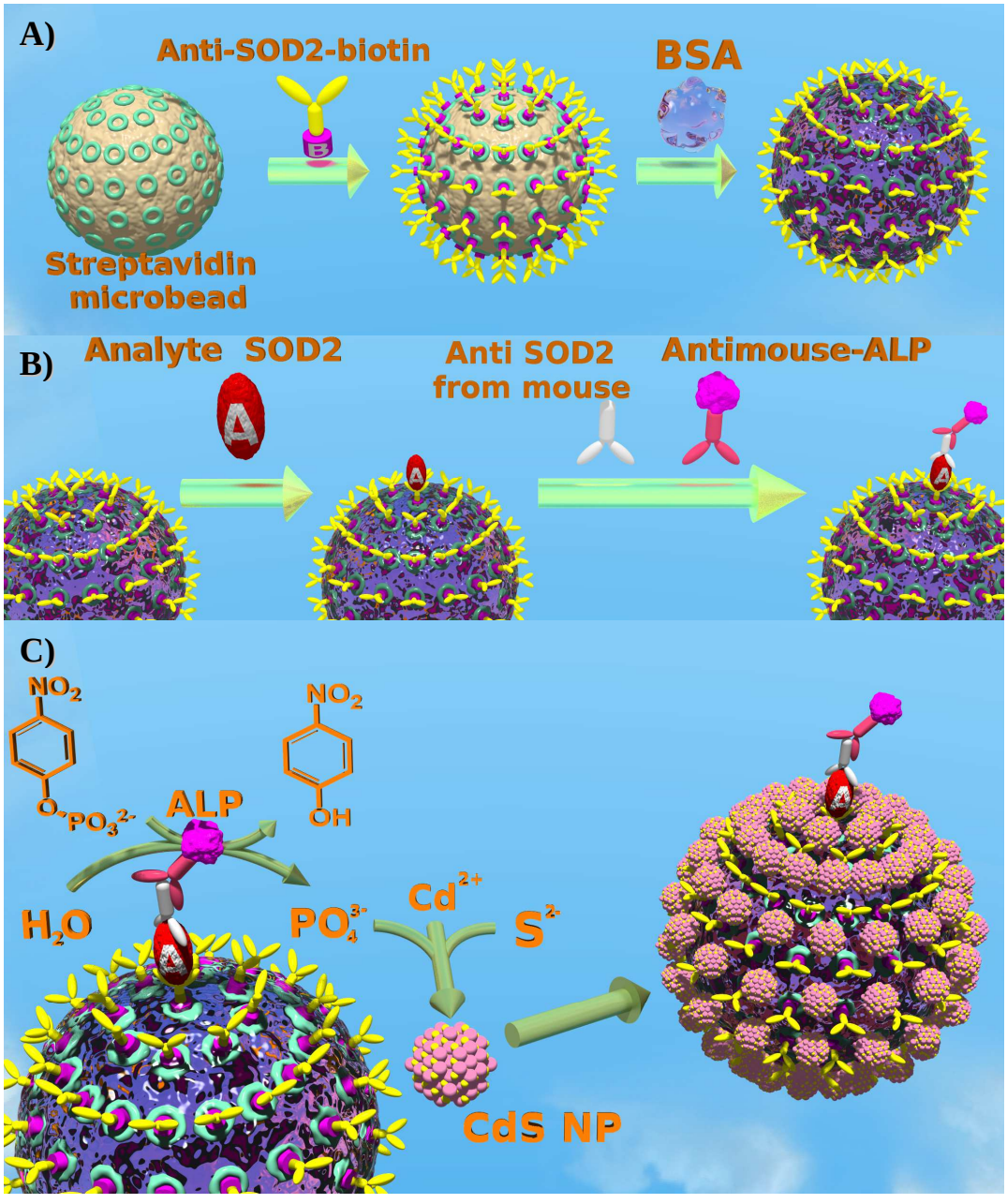

In the past we demonstrated that orthophosphate ions (PO_4^{3-}) produced by ALP stabilize CdS NPs produced from Na_2S and $Cd(NO_3)_2$ in situ.[27] Scheme 1C outlines the biocatalytic signal amplification cascade for detection of analyte SOD2 by the enzymatic production of CdS QDs in situ. As demonstrated in Scheme 1C, ALP captured on the microbeads due to the recognition event hydrolyzes para-nitrophenylphosphate (pNPP) to para-nitrophenol and orthophosphate ions which stabilize CdS NPs produced in situ by the interaction of Cd^{2+} with S^{2-} ions. The optimum concentrations of $Cd(NO_3)_2$ was 2.5 mM and Na_2S was 0.05 mM as shown in Figure S2.

ALP demonstrates the highest specific activity at basic pH in the presence of Mg^{2+} cations. On the other hand CdS NPs capped by negative PO_4^{-3} anions are more stable at basic pH which shifts the following three equilibriums to the right increasing the total stabilizing negative charge on QDs:

$H_3PO_4 \leftrightarrow H_2PO_4^- + H^+$

$H_2PO_4^- \leftrightarrow HPO_4^{-2} + H^+$

$HPO_4^{-2} \leftrightarrow PO_4^{-3} + H^+$

Therefore we used 50 mM Tris-HCl buffer containing 1 mM $MgCl_2$ with pH 8.8 for the enzymatic growth of CdS QDs. The resulting CdS NPs bind to the surface of microbeads, as confirmed by the experimental characterization of the microbeads.

Characterization of microbeads. In order to confirm the presence of the generated CdS NPs on the surface of the microbeads a wide field fluorescence microscope and a transmission electron microscopy (TEM) equipped with an Energy Dispersive X-Ray Spectrometer (EDX) were used. Fluorescence imaging analysis confirms the presence of CdS NPs on the surface of microspheres (**Figure 1**). In the absence of SOD2 no fluorescence was detected (**Figure 1A)**. In the images

obtained in the presence of 111.5 ng mL^{-1} SOD2, high fluorescence intensity was observed due to the adsorption of enzymatically generated CdS NPs on the surface of microbeads.

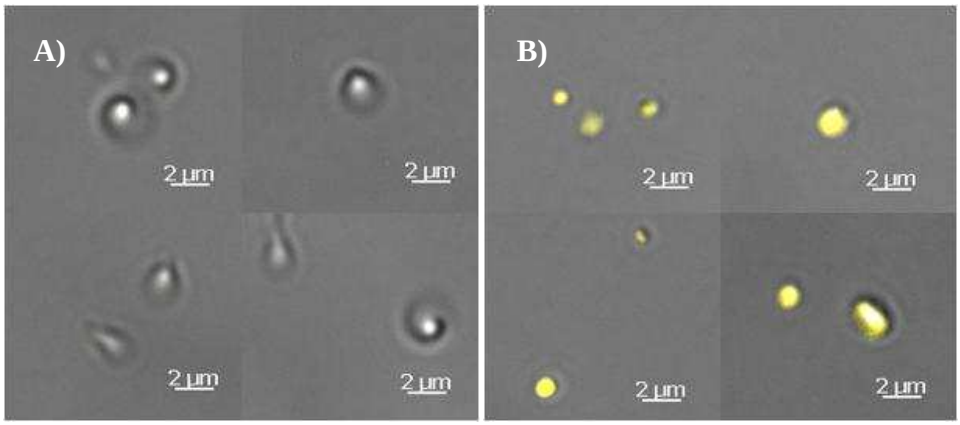

Figure 1. Fluorescence microscope images obtained (four different pictures in different areas of each sample were taken): (A) in the absence of SOD2 protein; (B) in the presence of SOD2 protein.

EDX spectra have been acquired in a transmission electron microscope (TEM) in scanning mode (STEM). Detected Cd was found to be colocalized with the microbeads for SOD2 treated samples (**Figure 2**). In the absence of SOD2 protein in the assay no Cd was detected. The present, low EDX signal was proven to be in this case noise only, and thus no image is shown for this sample (the EDX data analysis is presented in the supplementary information).

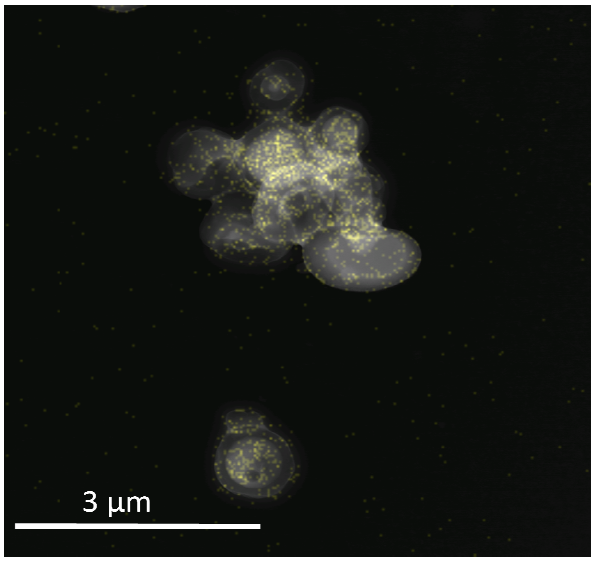

Figure 2. Overlay of detected Cd signal to the corresponding STEM image (20.000 magnification). The excitation occurred where the organic matrix is localized.

Scheme 2. Fluorogenic Detection Method

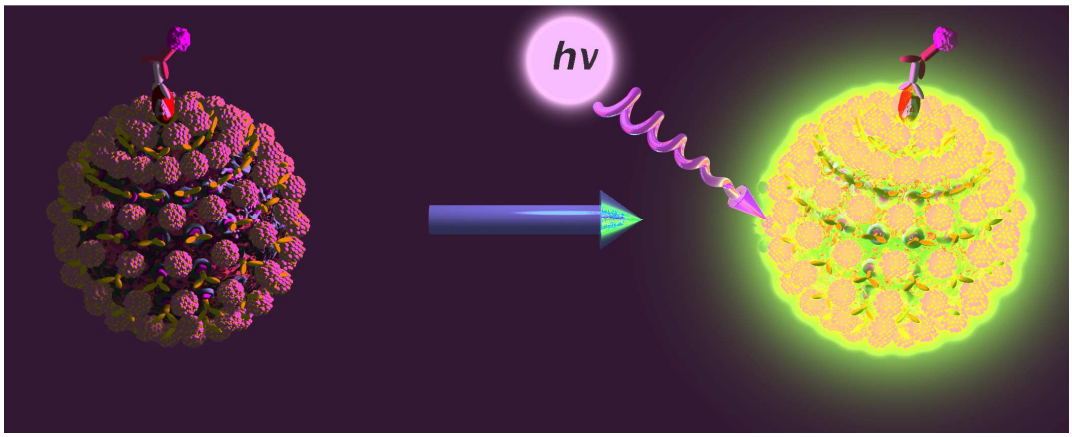

Three different analytical methods: fluorogenic, chromogenic and electrochemical, were used to follow the readout signal. **Scheme 2** represents the fluorogenic test, where CdS QDs immobilized on the surface of microbeads emit fluorescence under excitation with 320 nm light. **Figure 3A** represents fluorescence emission spectra of CdS QDs corresponding to different concentrations of SOD2 (from 0 to 111.6 ng mL^{-1}) in buffer solutions. The increase in the amount of adsorbed SOD2 protein leads to a rising fluorescence intensity. The received calibration curve in **Figure 3B** demonstrates that the intensity of the emission peaks increases with the concentration of the SOD2 protein. The response to varying SOD2 concentrations shows linearity from 0 to 11 ng mL^{-1} and saturation starting from 80 ng mL^{-1} SOD2 concentration. According to the calibration curve the limit of SOD2 detection was found to be 0.52 ng mL^{-1} (2.31 x 10^{-11} M).

Furthermore, we compared the performance of the fluorogenic method with that of the standard immunoassay based on the enzymatic hydrolysis of chromogenic substrate pNPP, followed by UV−Vis spectroscopy (**Figure 3C**). A linear response range for detection of SOD2 by this

method was between 0 ng mL^{-1} and 11 ng mL^{-1} and it shows the same value compared with the fluorogenic one. However, the lowest concentration of SOD2 that could be detected by this chromogenic system was found to be 1.307 ng mL^{-1} (5.82 x 10^{-11} M), which is 2.5 times worse than that of the fluorogenic assay.

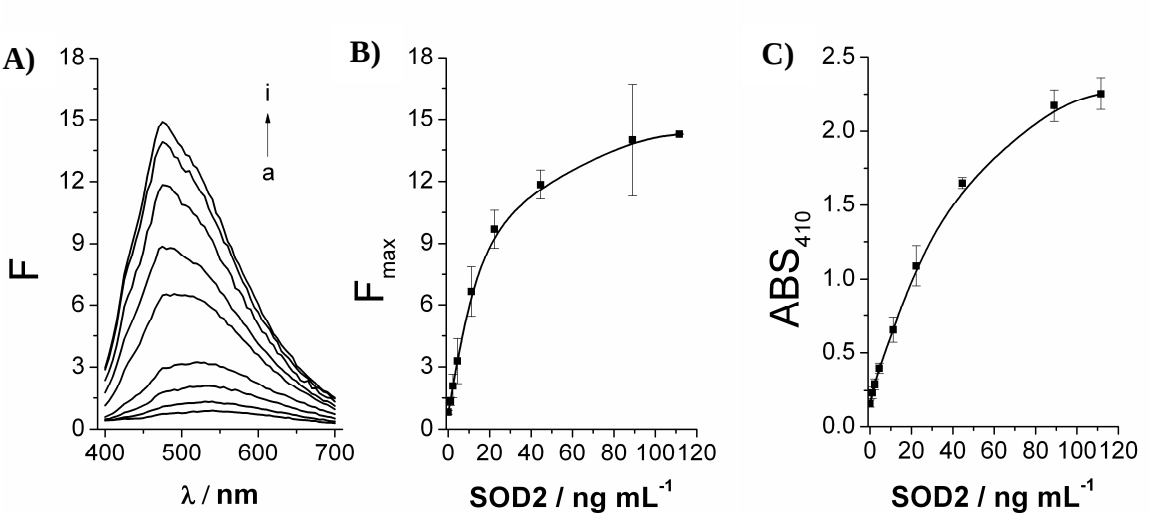

Figure 3. (A) Fluorescence emission spectra of the system containing: $Cd(NO_3)_2$ (2.5 mM), Na_2S (0.05 mM), pNPP (0.5 mM) and various concentrations of SOD2: (a) 0 ng mL^{-1}; (b) 1.1 ng mL^{-1}; (c) 2.23 ng mL^{-1}; (d) 4.46 ng mL^{-1}; (e) 11.16 ng mL^{-1}; (f) 22.3 ng mL^{-1}; (g) 44.6 ng mL^{-1}; (h) 89 ng mL^{-1}; and (i) 111.6 ng mL^{-1}. (B) Calibration curve of SOD2 obtained using maximum fluorescence intensity of the peak, F_{max}. (C) Calibration curve of SOD2 obtained using λ_{abs} = 410

Electrochemical detection of SOD2. Under the optimized operating conditions (step potential, amplitude and frequency), a series of different concentrations of enzymatically generated CdS NPs corresponding to SOD2 concentrations from 0 to 111.6 ng mL^{-1} was measured. Before performing the electrochemical studies, free exogenous cadmium ions which were not immobilized as CdS NPs on the surface of microbeads were washed off by ultrafiltration. Finally, the microbeads bearing CdS NPs were recovered and treated with hydrochloride acid to

now dissolve the cadmium from the NPs as it is depicted in **Scheme 3**. Like this we exclusively made available for the electrochemical detection only the cadmium which before formed QDs.

Scheme 3. Electrochemical Detection Method Using Screen Printed Electrodes

The mechanism of Cd^{2+} ions detection consists of several steps: accumulation, reduction and stripping stages as described below:

$$CdS\ NPs + 2HCl \xrightarrow{acid\ attack} Cd^{2+}\ (dis) + 2Cl^{-} + H_2S\uparrow$$

$$Cd^{2+}\ (dis) + 2e^{-} \xrightarrow{deposition\ (-1.2\ V\ vs.\ Ag/AgCl)} Cd(SPE)$$

$$Cd(SPE) \xrightarrow{SWV\ (-0.9\ V\ vs.\ Ag/AgCl)} Cd^{2+}\ (dis) + 2e^{-}$$

Firstly, the dissolved Cd^{2+} ions were reduced at -1.2 V *vs.* Ag/AgCl and electrochemically deposited on the surface of working electrode of disposable SPE. Subsequently, the deposited cadmium was electrochemically oxidized at -0.90 V *vs.* Ag/AgCl. The electrochemical signal increased during selective electrodeposition of cadmium ions corresponding to the increasing amounts of SOD2. Well-defined stripping peaks with maximum currents increasing in proportion to the concentration of SOD2 were observed at -0.90 V *vs.* Ag/AgCl as shown in stripping curves of **Figure 4A**. The square-wave voltammograms demonstrated four times wider linearity (up to 45 ng mL^{-1} **Figure 4B**) in comparison with that of the fluorogenic assay. It was confirmed that all the dissolved Cd^{2+} ions were deposited on the surface of the SPE (**Figure S4**). Fluorescence quenching phenomenon is usually observed upon aggregation of CdS NPs as has been reported in the literature.[44, 45] So, enzymatically generated CdS NPs partially lose fluorescence upon aggregation on microbeads, resulting in narrower linear range demonstrated by the fluorogenic assay. We explained the wider linearity of the electrochemical method by the fact that the electrochemical SWV readout signal depends only on the total amount of Cd^{2+} ions captured on microbeads in CdS and is not affected by the quenching due to quantum interaction between neighboring QDs. The lowest amount of SOD2 that could be detected by electrochemical method was found to be 0.44 ng mL^{-1} (1.96 x 10^{-11} M). The average relative standard deviation (RSD) calculated from the SOD2 calibration (obtained using at least three independent measurements) was 6.75%. The previously published various assays for superoxide dismutase demonstrated much worse detection limits than our electrochemistry detection immunoassay.

The electrochemical oxygen probe showed a detection limit of 1.5 x 10^{-9} M,[46] and two assays using surface plasma resonance (SPR) had detection limits of 1 x 10^{-9} M [47] and 0.9 x 10^{-6} M.[48]

The chromogenic ELISA employing HRP-antibody conjugate and 3,3',5,5'-tetramethylbenzidine gave a detection limit of 1.2 x 10^{-6} M and requires at least 6 h.[48] The most recent electrochemical method for detection of superoxide dismutase using affinity interaction has detection limit of 0.5 nM.[49] Thus, our fluorogenic and electrochemical assays requiring between 4 and 6 h of total incubation and washing time improve upon these published detection limits by three orders of magnitude. This remarkable decrease in the detection limit will allow for smaller samples needed from patients.

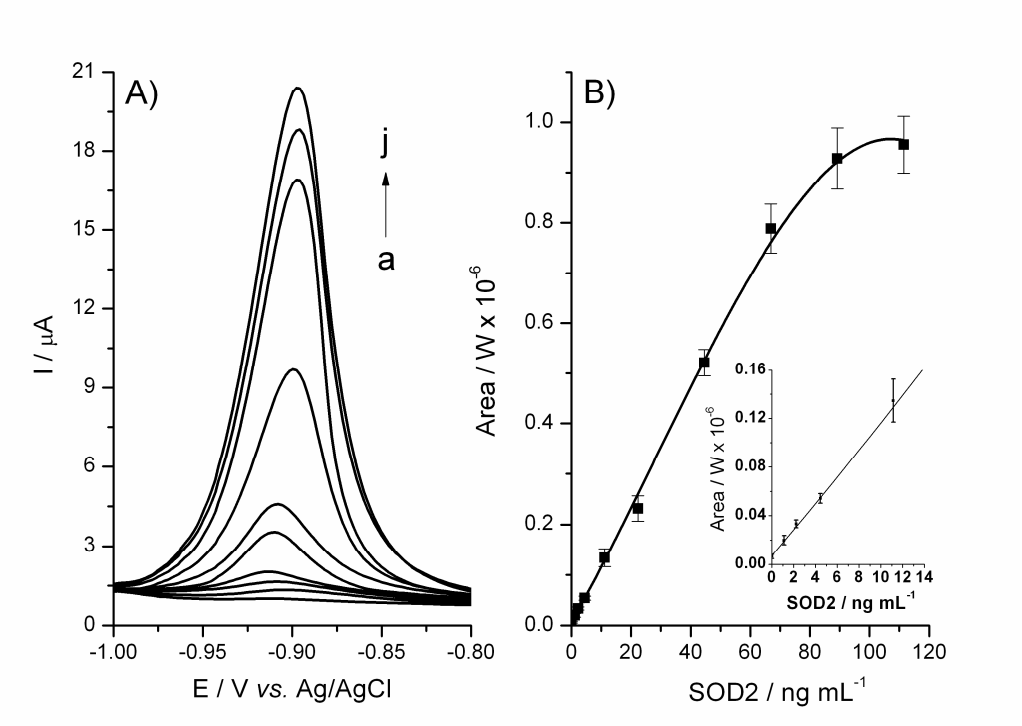

Figure 4. (A) Square wave voltammograms obtained for the SOD2 detection at different concentrations of (a) 0 ng mL^{-1}, (b) 1.12 ng mL^{-1}, (c) 2.23 ng mL^{-1}, (d) 4.46 ng mL^{-1}, (e) 11.15 ng mL^{-1}, (f) 22.30 ng mL^{-1}, (g) 44.60 ng mL^{-1}, (h) 66.90 ng mL^{-1}, (i) 89.20 ng mL^{-1} and (j) 111.50 ng mL^{-1}. (B) Calibration curve of SOD2 obtained using integrated area under peaks. Inset: Part of the calibration plot at low concentrations.

Finally, the detection of tumor markers in real samples is really of importance and gives information of the disease stage. For that reason, we also evaluated our assay for detection of SOD2 in HepG2 cell lysate samples. We validated the developed electrochemical method by running assays employing HepG2 cell lysate samples containing different known concentrations (spiked concentration: 0, 11.15, 22.30 and 44.60 ng mL^{-1}) of SOD2, which demonstrated the voltammetric curves depicted in **Figure 5A**. The calibration plot including the error bars for three different measurements (RSD = 7%) is also shown in **Figure 5B**. The similar calibration curves for SOD2 detection in buffer (dashed line) and cell lysate (dark line) demonstrate the suitability of the method for use in real samples.

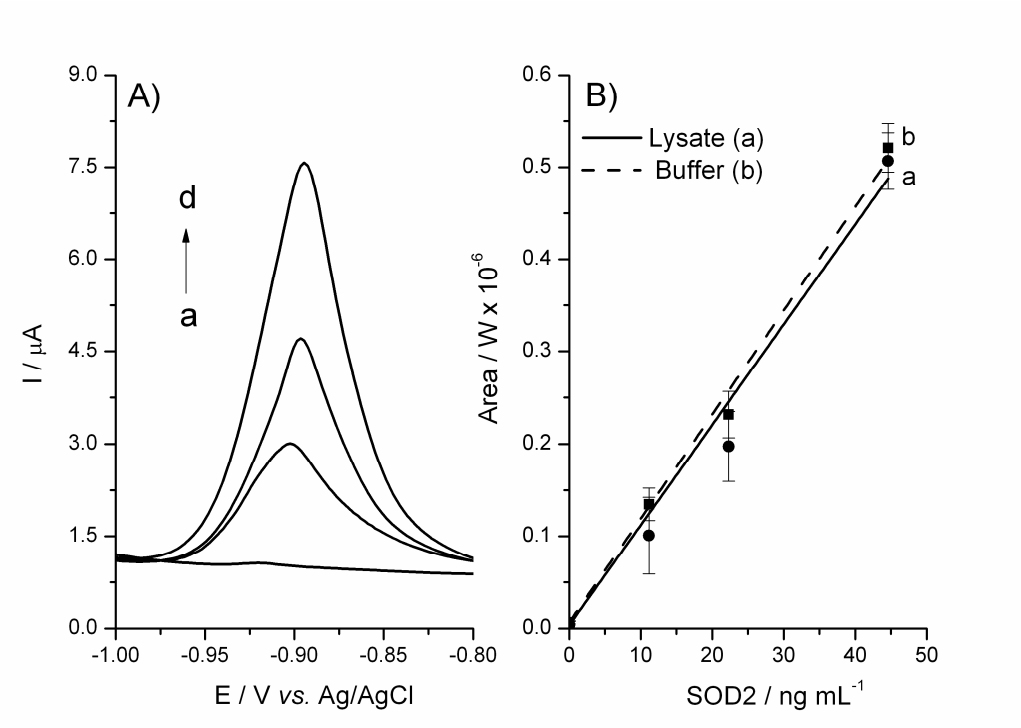

Figure 5. (A) Square wave voltammograms obtained using HepG2 cell lysate samples containing various SOD2 amounts: (a) 0 ng mL^{-1}, (b) 11.15 ng mL^{-1}, (c) 22.30 ng mL^{-1} and (d) 44.60 ng mL^{-1}. (B) Calibration curve of SOD2 in lysate (dark line) and buffer (dashed line) obtained using integrated area under peaks.

CONCLUSIONS

We developed a bead-based immunoassay for the detection of tumor biomarkers such as SOD2 employing enzymatic in situ generation and immobilization of CdS QDs onto microspheres. We have demonstrated that electrochemical and fluorogenic detection employing enzymatically generated CdS NPs yield new immunoassays with better detection limits in comparison with those of the previously published methods at least by three orders of magnitude. The electrochemical detection immunoassay did not suffer from signal loss due to aggregation of CdS NPs on microbeads and showed four times wider linear range than that of the fluorogenic immunoassay. Our methodology allows for the detection of SOD2 in lysates from HepG2 cells.

Enzymatic formation of QDs in situ enables employment of various physical methods such as fluorescence spectroscopy and electrochemistry to follow the readout signals and significantly improves the detection limit of immunoassays.

Thus, Microbead QD-ELISA, developed by us, can be applied with ultra high sensitivity in both detection systems, optical and electrochemical. While the optical characteristics of QDs made them well known, their electrochemical characteristics are not of any less power in Microbead QD-ELISA especially because of the wider linear response.

ASSOCIATED CONTENT

Supporting Information.

The supporting information is available free of charge via the Internet at http://pubs.acs.org.".
It contains plots related with the optimization of $Cd(NO_3)_2$ and Na_2S concentrations employed for in situ formation of CdS NPs and square wave voltammograms obtained from washings of

waste solutions. In addition it includes the characterization of microbeads bearing CdS NPs with STEM and EDX study. Confirmation of Cd^{2+} ions deposition on SPE.

AUTHOR INFORMATION

Corresponding Author

*V.P.: e-mail, vpavlov@cicbiomagune.es.

Author Contributions

The manuscript was written through contributions of all authors. All authors have given approval to the final version of the manuscript.

ACKNOWLEDGMENT

This work was supported by the Spanish Ministry of Economy and Competitiveness (Projects BIO2014-59741-R).

REFERENCES

(1) Shlyahovsky, B.; Pavlov, V.; Kaganovsky, L.; Willner, I., Biocatalytic Evolution of a Biocatalyst Marker: Towards the Ultrasensitive Detection of Immunocomplexes and DNA Analysis. *Angew. Chem., Int. Ed.* **2006,** 45, (29), 4815-4819.

(2) Pavlov, V.; Xiao, Y.; Shlyahovsky, B.; Willner, I., Aptamer-Functionalized Au Nanoparticles for the Amplified Optical Detection of Thrombin. *J. Am. Chem. Soc.* **2004,** 126, (38), 11768-11769.

(3) Garai-Ibabe, G.; Grinyte, R.; Golub, E. I.; Canaan, A.; de la Chapelle, M. L.; Marks, R. S.; Pavlov, V., Label Free and Amplified Detection of Cancer Marker EBNA-1 by DNA Probe based biosensors. *Biosens. Bioelectron.* **2011,** 30, (1), 272-275.

(4) Elmlund, L.; Kack, C.; Aastrup, T.; Nicholls, I., Study of the Interaction of Trastuzumab and SKOV3 Epithelial Cancer Cells Using a Quartz Crystal Microbalance Sensor. In 2015; Vol. 15, p 5884.

(5) Suriyanarayanan, S.; Nawaz, H.; Ndizeye, N.; Nicholls, I., Hierarchical Thin Film Architectures for Enhanced Sensor Performance: Liquid Crystal-Mediated Electrochemical Synthesis of Nanostructured Imprinted Polymer Films for the Selective Recognition of Bupivacaine. In 2014; Vol. 4, p 90.

(6) Sakamoto, S.; Sakoda, J.; Morinaga, O.; Waraporn, P.; Tsuchihashi, R.; Morimoto, S.; Kinjo, J.; Tanaka, H., Development of an Enzyme Linked Immunosorbent Assay for Direct Determination of Anticancer Drug Vitamin K3 in Serum. *J. Health Sci.* **2008,** 54, (4), 508-511.

(7) Phrompittayarat, W.; Putalun, W.; Tanaka, H.; Wittaya-Areekul, S.; Jetiyanon, K.; Ingkaninan, K., An Enzyme-Linked Immunosorbant Assay Using Polyclonal Antibodies against Bacopaside I. *Anal. Chim. Acta.* **2007,** 584, (1), 1-6.

(8) Sakamoto, S.; Putalun, W.; Tsuchihashi, R.; Morimoto, S.; Kinjo, J.; Tanaka, H., Development of an Enzyme-Linked Immunosorbent Assay (ELISA) Using Highly-Specific Monoclonal Antibodies against Plumbagin. *Anal. Chim. Acta.* **2008,** 607, (1), 100-5.

(9) Thacker, J. D.; Casale, E. S.; Tucker, C. M., Immunoassays (ELISA) for Rapid, Quantitative Analysis in the Food-Processing Industry. *J. Agric. Food Chem.* **1996,** 44, (9), 2680-2685.

(10) Medina-Sánchez, M.; Miserere, S.; Morales-Narváez, E.; Merkoçi, A., On-Chip Magneto-Immunoassay for Alzheimer's Biomarker Electrochemical Detection by Using Quantum Dots as Labels. *Biosens. Bioelectron.* **2014,** 54, 279-284.

(11) Ho, T. Y. J.; Chan, C.-C.; Chan, K.; Wang, Y. C.; Lin, J.-T.; Chang, C.-M.; Chen, C.-S., Development of a Novel Bead-Based 96-Well Filtration Plate Competitive Immunoassay for the Detection of Gentamycin. *Biosens. Bioelectron.* **2013,** 49, 126-132.

(12) Jiang, D.; Zhu, P.; Jiang, H.; Ji, J.; Sun, X.; Gu, W.; Zhang, G., Fluorescent Magnetic Bead-Based Mast Cell Biosensor for Electrochemical Detection of Allergens in Foodstuffs. *Biosens. Bioelectron.* **2015,** 70, 482-490.

(13) Zhang, H.; Liu, L.; Fu, X.; Zhu, Z., Microfluidic Beads-Based Immunosensor for Sensitive Detection of Cancer Biomarker Proteins Using Multienzyme-Nanoparticle Amplification and Quantum Dots Labels. *Biosens. Bioelectron.* **2013,** 42, 23-30.

(14) Tekin, H. C.; Gijs, M. A. M., Ultrasensitive Protein Detection: a Case for Microfluidic Magnetic Bead-Based Assays. *Lab Chip* **2013,** 13, (24), 4711-4739.

(15) Katz, E.; Willner, I., Integrated Nanoparticle–Biomolecule Hybrid Systems: Synthesis, Properties, and Applications. *Angew. Chem., Int. Ed.* **2004,** 43, (45), 6042-6108.

(16) Liz-Marzán, L. M., Nanometals: Formation and Color. *Mater. Today* **2004,** 7, (2), 26-31.

(17) Sperling, R. A.; Rivera Gil, P.; Zhang, F.; Zanella, M.; Parak, W. J., Biological Applications of Gold Nanoparticles. *Chem. Soc. Rev.* **2008,** 37, (9), 1896-1908.

(18) Xiao, Y.; Pavlov, V.; Levine, S.; Niazov, T.; Markovitch, G.; Willner, I., Catalytic Growth of Au Nanoparticles by NAD(P)H Cofactors: Optical Sensors for NAD(P)+-Dependent Biocatalyzed Transformations. *Angew. Chem., Int. Ed.* **2004,** 43, (34), 4519-4522.

(19) Shlyahovsky, B.; Katz, E.; Xiao, Y.; Pavlov, V.; Willner, I., Optical and Electrochemical Detection of NADH and of NAD+-Dependent Biocatalyzed Processes by the Catalytic Deposition of Copper on Gold Nanoparticles. *Small* **2005,** 1, (2), 213-216.

(20) Pavlov, V., Enzymatic Growth of Metal and Semiconductor Nanoparticles in Bioanalysis. *Part. Part. Syst. Charact.* **2013,** 31, (1), 36-45.

(21) Saa, L.; Virel, A.; Sanchez-Lopez, J.; Pavlov, V., Analytical Applications of Enzymatic Growth of Quantum Dots. *Chemistry* **2010,** 16, (21), 6187-92.

(22) Saa, L.; Mato, J. M.; Pavlov, V., Assays for Methionine Gamma-Lyase and S-Adenosyl-L-Homocysteine Hydrolase Based on Enzymatic Formation of CdS Quantum Dots in situ. *Anal. Chem.* **2012,** 84, (21), 8961-8965.

(23) Saa, L.; Pavlov, V., Enzymatic Growth of Quantum Dots: Applications to Probe Glucose Oxidase and Horseradish Peroxidase and Sense Glucose. *Small* **2012,** 8, (22), 3449-3455.

(24) Garai-Ibabe, G.; Saa, L.; Pavlov, V., Enzymatic Product-Mediated Stabilization of CdS Quantum Dots Produced in situ: Application for Detection of Reduced Glutathione, NADPH, and Glutathione Reductase Activity. *Anal. Chem.* **2013,** 85, (11), 5542-5546.

(25) Garai-Ibabe, G.; Saa, L.; Pavlov, V., Thiocholine Mediated Stabilization of in situ Produced CdS Quantum Dots:Aapplication for the Detection of Acetylcholinesterase Activity and Inhibitors. *Analyst* **2014,** 139, (1), 280-284.

(26) Grinyte, R.; Saa, L.; Garai-Ibabe, G.; Pavlov, V., Biocatalytic Etching of Semiconductor Cadmium Sulfide Nanoparticles as a New Platform for the Optical Detection of Analytes. *Chem. Commun.* **2015,** 51, (96), 17152-17155.

(27) Malashikhina, N.; Garai-Ibabe, G.; Pavlov, V., Unconventional Application of Conventional Enzymatic Substrate: First Fluorogenic Immunoassay Based on Enzymatic Formation of Quantum Dots. *Anal. Chem.* **2013,** 85, (14), 6866-6870.

(28) Dong, X.-Y.; Mi, X.-N.; Zhao, W.-W.; Xu, J.-J.; Chen, H.-Y., CdS Nanoparticles Functionalized Colloidal Carbon Particles: Preparation, Characterization and Application for Electrochemical Detection of Thrombin. *Biosens. Bioelectron.* **2011,** 26, (8), 3654-3659.

(29) Sharma, A.; Rao, V. K.; Kamboj, D. V.; Gaur, R.; Upadhyay, S.; Shaik, M., Relative Efficiency of Zinc Sulfide (ZnS) Quantum Dots (QDs) Based Electrochemical and Fluorescence Immunoassay for The Detection of Staphylococcal Enterotoxin B (SEB). *J. Appl. Biotechnol. Rep.* **2015,** 6, 129-136.

(30) Kong, F.-Y.; Xu, B.-Y.; Xu, J.-J.; Chen, H.-Y., Simultaneous Electrochemical Immunoassay Using CdS/DNA and PbS/DNA Nanochains as Labels. *Biosens. Bioelectron.* **2013,** 39, (1), 177-182.

(31) Sharma, A.; Rao, V. K.; Kamboj, D. V.; Upadhyay, S.; Shaik, M.; Shrivastava, A. R.; Jain, R., Sensitive Detection of Staphylococcal Enterotoxin B (SEB) Using Quantum Dots by Various Methods with Special Emphasis on an Electrochemical Immunoassay Approach. *RSC Advances* **2014,** 4, (64), 34089-34095.

(32) Monton, H.; Parolo, C.; Aranda-Ramos, A.; Merkoci, A.; Nogues, C., Annexin-V/Quantum Dot Probes for Multimodal Apoptosis Monitoring in Living Cells: Improving Bioanalysis Using Electrochemistry. *Nanoscale* **2015,** 7, (9), 4097-4104.

(33) Haram, S. K.; Quinn, B. M.; Bard, A. J., Electrochemistry of CdS Nanoparticles: A Correlation between Optical and Electrochemical Band Gaps. *J. Am. Chem. Soc.* **2001,** 123, (36), 8860-8861.

(34) Bae, Y.; Myung, N.; Bard, A. J., Electrochemistry and Electrogenerated Chemiluminescence of CdTe Nanoparticles. *Nano Lett.* **2004,** 4, (6), 1153-1161.

(35) Chen, A.; Shah, B., Electrochemical Sensing and Biosensing Based on Square Wave Voltammetry. *Anal. Methods* **2013,** 5, (9), 2158-2173.

(36) Huang, H.; Zhu, J.-J., The Electrochemical Applications of Quantum Dots. *Analyst* **2013,** 138, (20), 5855-5865.

(37) Arben Merkoçi and Luiz Humberto Marcolino-Junior and Sergio Marín and Orlando Fatibello-Filho and Salvador, A., Detection of Cadmium Sulphide Nanoparticles by Using Screen-Printed Electrodes and a Handheld Device. *Nanotechnology* **2007,** 18, (3), 035502.

(38) Escamilla-Gómez, V.; Hernández-Santos, D.; González-García, M. B.; Pingarrón-Carrazón, J. M.; Costa-García, A., Simultaneous Detection of Free and Total Prostate Specific Antigen on a Screen-Printed Electrochemical Dual Sensor. *Biosens. Bioelectron.* **2009,** 24, (8), 2678-2683.

(39) McCord, J. M.; Fridovich, I., Superoxide dismutase. An Enzymic Function for Erythrocuprein (hemocuprein). *J. Biol. Chem.* **1969,** 244, (22), 6049-6055.

(40) Weydert, C. J.; Waugh, T. A.; Ritchie, J. M.; Iyer, K. S.; Smith, J. L.; Li, L.; Spitz, D. R.; Oberley, L. W., Overexpression of Manganese or Copper-Zinc Superoxide Dismutase Inhibits Breast Cancer Growth. *Free Radical Biol. Med.* **2006,** 41, (2), 226-237.

(41) Li, N.; Oberley, T. D.; Oberley, L. W.; Zhong, W., Overexpression of Manganese Superoxide Dismutase in DU145 Human Prostate Carcinoma Cells has Multiple Effects on Cell Phenotype. *Prostate* **1998,** 35, (3), 221-233.

(42) Zhao, Y.; Xue, Y.; Oberley, T. D.; Kiningham, K. K.; Lin, S. M.; Yen, H. C.; Majima, H.; Hines, J.; St Clair, D., Overexpression of Manganese Superoxide Dismutase Suppresses

Tumor Formation by Modulation of Activator Protein-1 Signaling in a Multistage Skin Carcinogenesis Model. *Cancer Res.* **2001,** 61, (16), 6082-6088.

(43) Cullen, J. J.; Weydert, C.; Hinkhouse, M. M.; Ritchie, J.; Domann, F. E.; Spitz, D.; Oberley, L. W., The Role of Manganese Superoxide Dismutase in the Growth of Pancreatic Adenocarcinoma. *Cancer Res.* **2003,** 63, (6), 1297-1303.

(44) Noh, M.; Kim, T.; Lee, H.; Kim, C.-K.; Joo, S.-W.; Lee, K., Fluorescence Quenching caused by Aggregation of Water-Soluble CdSe Quantum Dots. *Colloids Surf., A* **2010,** 359, (1-3), 39-44.

(45) Kang, T.; Um, K.; Park, J.; Chang, H.; Lee, D. C.; Kim, C.-K.; Lee, K., Minimizing the Fluorescence Quenching Caused by Uncontrolled Aggregation of CdSe/CdS Core/Shell Quantum Dots for Biosensor Applications. *Sens. Actuators, B* **2016,** 222, 871-878.

(46) Moscone, D.; Mascini, M., Determination of Superoxide Dismutase Activity with an Electrochemical Oxygen Probe. *Anal. Chim. Acta* **1988,** 211, 195-204.

(47) Ivansson, D.; Bayer, K.; Mandenius, C.-F., Quantitation of Intracellular Recombinant Human Superoxide Dismutase Using Surface Plasmon Resonance. *Anal. Chim. Acta* **2002,** 456, (2), 193-200.

(48) Vostiar, I.; Tkac, J.; Mandenius, C.-F., Intracellular Monitoring of Superoxide Dismutase Expression in an Escherichia Coli Fed-Batch Cultivation Using on-line Disruption with at-Line Surface Plasmon Resonance Detection. *Anal. Biochem.* **2005,** 342, (1), 152-159.

(49) Santharaman, P.; Das, M.; Singh, S. K.; Sethy, N. K.; Bhargava, K.; Claussen, J. C.; Karunakaran, C., Label-Free Electrochemical Immunosensor for the Rapid and Sensitive Detection of the Oxidative Stress Marker Superoxide Dismutase 1 at the Point-of-Care. *Sens. Actuators, B* **2016,** 236, 546-553.

Table of Contents